Water Resour Manage
DOI 10.1007/s11269-016-1364-0

Development of a Glacio-hydrological Model for Discharge and Mass Balance Reconstruction

Rajesh Kumar[1] · **Shaktiman Singh**[1] · **Ramesh Kumar**[1] · **Atar Singh**[1] · **Anshuman Bhardwaj**[1,2] · **Lydia Sam**[1,3] · **Surjeet Singh Randhawa**[4] · **Akhilesh Gupta**[5]

Received: 10 October 2015 / Accepted: 18 May 2016

Abstract The reconstruction of glacio-hydrological records for the data deficient Himalayan catchments is needed in order to study the past and future water availability. The study provides outcomes of a glacio-hydrological model based on the degree-day approach. The model simulates the discharge and mass balance for glacierised Shaune Garang catchment. The degree-day factors for different land covers, used in the model, were estimated using daily stake measurements on Shaune Garang glacier and they were found to be varying between 2.6 ± 0.4 and 9.3 ± 0.3 mm °C^{-1}day^{-1}. The model is validated using observed discharge during ablation season of 2014 with coefficient of determination (R^2) 0.90 and root mean square error (RMSE) 1.05 m^3 sec^{-1}. The model is used to simulate discharge from 1985 to 2008 and mass balance from 2001 to 2008. The model results show significant contribution of seasonal snow and ice melt in total discharge of the catchment, especially during summer. We observe the maximum discharge in July having maximum contribution from snow and ice melt. The annual melt season discharge shows following a decreasing trend in the simulation period. The reconstructed mass balance shows mass loss of 0.89 m we per year between 2001 and 2008 with slight mass gain during 2000/01 and 2004/05 hydrological years.

✉ Shaktiman Singh
shaktiman.singh@hotmail.com

[1] Department of Environmental Science, School of Basic Sciences & Research, Sharda University, Greater Noida, India

[2] Department of Computer Science, Electrical and Space Engineering, Atmospheric Science Group, Luleå University of Technology, Kiruna, Sweden

[3] Defence Terrain Research Laboratory, New Delhi, India

[4] State Council for Science, Technology. & Environment, Shimla, India

[5] Department of Science & Technology, New Delhi, India

Published online: 30 May 2016

Keywords Debris cover · Degree-day factor · Discharge · Mass balance · Snow and ice melt · Water availability

1 Introduction

Mountains cover around 24 % of total global surface area and inhabit around 12 % of world's population (Schild 2008). Around 10 % of the total world's population is dependent on mountains directly for their livelihoods while another 40 % are dependent indirectly on them for timber and non-timber forest products, fresh water, and river valley projects for industrial, agricultural and domestic purposes (Schild 2008). These ecosystem services are not only relevant for inhabitants of the mountains, but also for those living in plains or coastal areas. The mountains of high Asia or Hindu Kush-Himalaya (HKH) have around 50 % of all the glacial area falling outside the polar region (Mayewski and Jeschke 1979). The total number of glaciers in the HKH region is 54252 which cover an area of around 60000 km^2 (Bajracharya and Shrestha 2011). The signatures of changing climate in terms of changes in temperature (Bhutiyani et al. 2007; Dimri and Dash 2012; Liu and Chen 2000; Shrestha et al. 1999), precipitation (Archer and Fowler 2004; Bhutiyani et al. 2010; Shrestha et al. 2000) and change in area and volume of glaciers (Bolch et al. 2012; Gardelle et al. 2013; Kääb et al. 2012; Shea et al. 2015) is evident in the Himalaya. However, these trends of changes vary temporally and spatially across the HKH due to the orographic complexity of the region (Arora et al. 2006; Basistha et al. 2008; Bookhagen and Burbank 2010). The changes in climate parameters, glacier area, and volume will in due course affect the supply of water downstream (Immerzeel et al. 2010; Lutz et al. 2014), influencing the livelihood and economy of the densely populated HKH region and downstream areas (Tiwari and Joshi 2012; Xu et al. 2009). The change in stream flow will also distress the sediment load (Jain et al. 2003) affecting the hydropower plants in downstream areas (Garg and Jothiprakash 2012). The proportion of melt contribution from snow and glacier ice increases with increasing altitude (Singh et al. 2008) and is a significant component of total stream flow in Himalayan rivers (Immerzeel et al. 2010; Singh et al. 2016). Therefore, accurate estimation of discharge from high altitude catchments depends on accurate estimation of melt from seasonal snow cover and ice (Hock 2003).

There are two main approaches to model melt from a glaicerised catchment namely energy balance approach and temperature index or degree-day approach (Hock 2003). The energy balance approach to estimate melt in a glacierised catchment requires several weather parameters (incoming and reflected shortwave radiation, downwelling long-wave radiation, air and surface temperature, relative humidity and wind speed and direction) collected on or near the glacier (Azam et al. 2014a; Fujita and Ageta 2000; Kayastha et al. 1999; Lejeune et al. 2013; Mölg et al. 2012; Zhang et al. 2013). However, such in situ parameters are very difficult to collect on a regular basis in the Himalaya. In such scenario, the temperature index or degree-day approach is more apt for the region as it is comparatively simple in computation and requires readily-available temperature data. In addition, despite its simplicity, the model gives competitive results with respect to energy balance models at catchment scale (Hock 2003). According to Ohmura (2001), air temperature is a good index for snow and ice melt estimation as it can be used as a proxy for the components of energy balance models such as, long-wave downwelling and absorbed shortwave radiation.

Due to computational simplicity and fewer input parameters, the degree-day approach has been widely used in mountainous catchments (Hock 2003). Many studies in the Himalayan region (Arora et al. 2008; Jain et al. 2010; Pradhananga et al. 2014; Li et al. 2015; Singh and Bengtsson 2003; Singh and Jain 2003; Singh et al. 2008) use degree-day approach to model melt-runoff satisfactorily.

Mass balance is an important climate indicator and is closely associated to temperature index models (Ohmura et al. 2007). These models have been previously used to estimate mass balance of glaciers (Bøggild et al. 1994; Braithwaite and Zhang 1999). Recently, Azam et al. (2014b) have reconstructed the mass balance of Chhota Shigri glacier in the western Himalaya using degree-day approach and they have found the reconstructed values to be in good accordance with observed glaciological mass balance. A recent study by Shea et al. (2015) has used modified degree-day model calibrated using geodetic mass change, glacier velocity and terminus fluctuation to model mass changes of glaciers in the Everest region.

Presently, the oversimplified empirical temperature index models are unable to model melt from debris-covered part of the glacier (Nicholson and Benn 2006; Juen et al. 2014) due to complex relationship between melting of ice under debris cover and altitude (Pratap et al. 2015; Srivastava et al. 2014). Another aspect, which is often ignored in such models, is the occurrence of both, solid and liquid precipitations in higher reaches of a catchment. The solid precipitation naturally results in a delayed discharge (Bookhagen and Burbank 2010) and the liquid precipitation results in increased melting (Singh 2001) and consequently discharge, which is often difficult to model. Therefore, such events should be closely recorded and incorporated in modelling runoff from a high altitude glacierised catchment.

In the present study, we are trying to address several existing research gaps in glacio-hydrological modelling of a debris-covered Himalayan catchment. The highlights of our study are: (1) long-term (1985–2008) melt season discharge simulations for debris-covered glacierised Shaune Garang catchment within the western Indian Himalaya, (2) mass balance reconstruction for the glacierised area in Shaune Garang catchment, (3) a first-time incorporation of melt factor estimates based on in situ measurements for debris-cover parts in different altitude ranges, and (4) inclusion of temporal seasonal snow and land cover areal changes for entire catchment as an input for reconstruction of mass balance and discharge. The overall objective of this study is to estimate discharge and mass balance of glacierised area in Shaune Garang catchment. We have used stake measurements on Shaune Garang glacier during ablation season of 2014 to compute degree-day factors separately for snow, ice and debris-covered ice surfaces. These inputs were used in a semi-distributed glacio-hydrological model which was validated against observed discharge (July, 2014 to September, 2014) and then was used to reconstruct long-term monthly discharge (1985–2008) and annual mass balance (2001–2008).

2 Study Area

Shaune Garang (31.25° to 31.38° N latitude and 78.25° to 78.41° E longitude) is a small glacierised catchment situated in the Pir Panjal range of Western Himalaya (Fig. 1). The catchment is influenced by westerlies during winter season, and Indian summer monsoon during summer season (Bookhagen and Burbank 2010). The catchment contributes its discharge to the Baspa river which is a second-order tributary to the Sutlej river. The total area of the Shaune Garang catchment is around 60 km^2. The area of the catchment above discharge gauge (3963 m asl) is 38.13 km^2, 24 % of which consist of four glaciers. Shaune Garang glacier (31.28° to 31.30° N latitude and 78.31° to 78.36° E longitude) is the largest glacier (4.94 km^2) in the catchment, and the main contributor of glacier-melt to total stream flow. The glaciers in the catchment are highly debris-covered, with a trend of gradually decreasing debris thickness with increasing altitude.

3 Data Used

3.1 Temperature and Precipitation

An automatic weather station (HOBO U-30 NRC, referred as 'AWS-1') was installed at an elevation 4569 m asl on lateral moraine near snout of the Shaune Garang glacier (Fig. 1). The temperature data was collected at hourly interval. This data was used for calculating daily mean temperature and degree-day factor for different land surfaces during the ablation season of 2014. Monthly temperature data collected at Rakchham (3045 m asl) from 1985 to 2007 was used for long term simulation of monthly discharge (Fig. 1). Another automatic weather station (Davis Vantage Pro-2, referred as 'AWS-2'), (Fig. 1) calibrated and validated with respect to AWS-1 under laboratory conditions, was installed at lower elevation (4166 m asl) for estimation of temperature gradient in the catchment which was found to be 0.0061 °C per meter on an average from July to September.

The monthly totals of precipitation data collected at AWS-1 were used in the model for the validation period. Due to unavailability of long-term observed precipitation (1985–2000) near

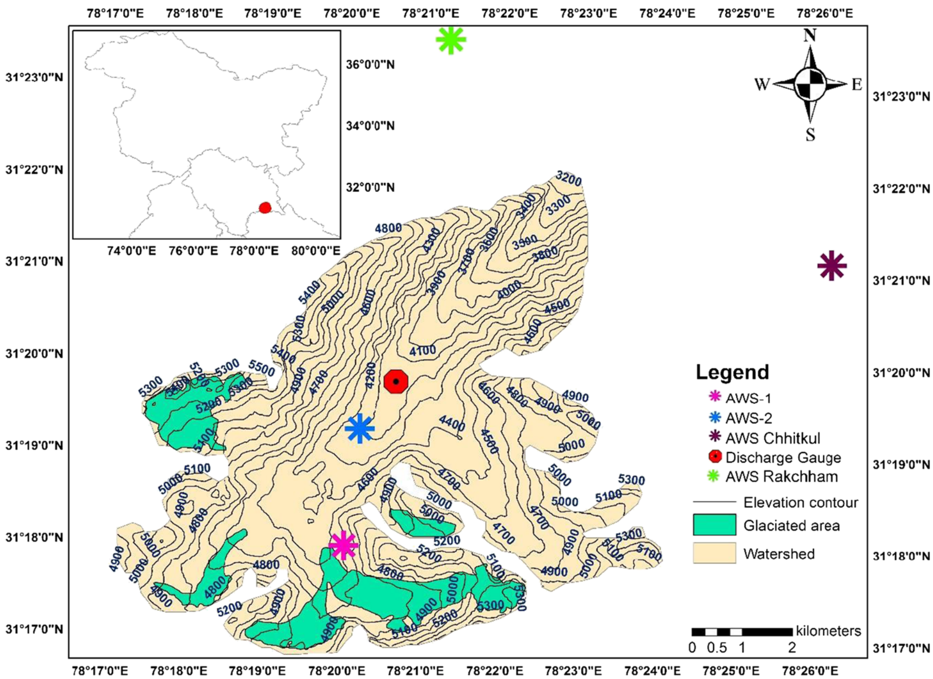

Fig. 1 Map showing location of Shaune Garang catchment and glacierised area in the catchment (Landsat 8, 20th August, 2014) with location of stations and discharge gauge

Table 1 Details of steps followed, parameters used each step, their source and period for which they have been used

Step	Parameter	Source	Period
Validation	Temperature	AWS-1	11 July to 27 September, 2014
	Precipitation	AWS-1	11 July to 27 September, 2014
	DDF	Temperature from AWS-1 and stake measurements	11 July to 27 September, 2014
Simulation	Temperature	Rakchham station	1985–2008
	Precipitation	Chhitkul station	2001–2008
	Precipitation	Bias-corrected (using daily data from Chhitkul station) APHRODITE data	1985–2000

the basin, gridded reanalysis precipitation data product Asian Precipitation – Highly Resolved Observational Data Integration towards Evaluation (APHRODITE) data (Yatagai et al. 2012) was used, which gives the competitive estimate for precipitation in Himalaya, with limited accuracy in high altitude (Andermann et al. 2011; Krakauer et al. 2013). APHRODITE has been used in other such studies in Himalaya (Panday et al. 2014; Shea et al. 2015). The daily precipitation product of APHRODITE (APHRO_MA_V1003R1) in comparison with daily sum of precipitation collected at Chhitkul (3462 m asl) (Fig. 1), showed significantly high estimates of precipitation, particularly in winter. Therefore, the precipitation recorded at Chhitkul from 2001 to 2008 was used to bias-correct the APHRODITE data using method suggested by Gudmundsson et al. (2012). The bias-corrected APHRODITE data was used for simulation period 1985–2000 while the precipitation data collected at Chhitkul station was used for simulation period 2001–2008.

Monthly precipitation sum from Rakchham and Chhitkul station was compared for the period January, 2005 to June, 2008 to estimate the precipitation gradient in the basin. The analysis shows that the precipitation in the basin increases at an average rate of 0.015 mm per meter. The temperature and precipitation data used in the study for different time periods has been summarised in Table 1.

3.2 Discharge Measurement

For measurement of discharge of Shaune Garang catchment, discharge gauging site was established at a distance of around 3 km from the snout of Shaune Garang glacier (4467 m asl) and at an elevation of 3963 m asl. The site chosen was suitable for discharge measurement due to low turbulence and comparatively more laminar flow. The discharge was measured using the area-velocity method (Eq. 1). The parameters used in the equation were estimated in the field following the procedure suggested by Herschy (1993).

$$Q_o = A_{cs} * v \tag{1}$$

Where,

Q_o observed discharge ($m^3 \ sec^{-1}$)
A_{cs} area of cross section of river bed (m^2)

v velocity of water (m sec^{-1})

In order to avoid the inclusion of errors due to any change in the cross-section area during the observation period, we measured the cross-section area of the river bed at regular intervals (thrice during the observation period). We further modified the measured cross-section area at daily resolution using manual measurement of water level, twice a day. The velocity of water was also measured twice daily (09:00 and 15:00 h), using Digital Metric Price type Current Meter (Make- Gurley Precision Instruments, USA, Model 622A).

3.3 Satellite Data

Elevation is a very important factor that governs changes in temperature, precipitation, and thus, melting. In the present study, the elevation information at various modelling stages was extracted from ASTER GDEM V2 of 30 m resolution. The catchment up to the discharge measurement site was divided into eight elevation zones with equal elevation difference of 200 m. The temporal land cover of the catchment was delineated using Landsat images for different acquisition dates, through manual digitization. We classified glacier covered area into ice, snow and debris cover, and glacier free area into snow and non-snow cover. There was a limited availability of seasonal snow-free and cloud-free images for the study area and we have tried to utilise images with minimum cloud cover for optimal mapping of land cover changes.

MODIS/Terra Snow Cover 8-Day L3 Global 500 m Grid product from 4 July 2002 to 23 October 2008 was used to estimate monthly average of snow cover in each elevation zone of the catchment (reported accuracy ~93 % by Hall and Riggs 2007). For the simulation period before 2002, cloud free Landsat images were used to obtain NDSI image based on the method proposed by Cea et al. (2007). The study suggests that the accuracy of using Landsat-derived NDSI for mapping snow cover is even better than the MODIS snow cover product. The snow covered area within a Himalayan catchment is primarily controlled by elevation and aspect (Jain et al. 2009). Therefore, multiple linear regression was used to develop an equation between month, temperature, and precipitation at each altitudinal band to estimate snow cover. The equation was then used for the estimation of snow cover for each altitudinal band for the months where cloud-free satellite images were not available.

The area of the catchment above discharge gauge is 38.13 km^2, out of which around 75 % is non-glacierised, 5 % debris-covered glacierised area and remaining 20 % is debris-free glacierised area. The comparison of area delineated from images of Landsat 3 (1980) and Landsat 8 (2014) shows reduction of glacierised area from 33 % in 1980 to 24 % in 2014 of the total catchment area above discharge gauge. The debris-covered fraction of the glacierised area in the catchment reduced from about 25 % in 1980 to 24 % in 2014. The area mapped using monthly images of Landsat 8 from July, 2014 to September, 2014 were used in the model for the validation period (Fig. 2). In the mass balance reconstruction of Chhota Shigri glacier by Azam et al. (2014b), the hypsometry of the glacier was assumed to be unchanged during 1969 to 2012 due to very less areal loss of glacier area mapped by Pandey and Venkataraman (2013) during 1988 to 2010.

Due to unavailability of continuous cloud-free images for the catchment, the simulation period was divided into three parts, 1985–1992, 1993–2000 and 2001–2008, with at least one seasonal snow and cloud-free scene as representative of each period.

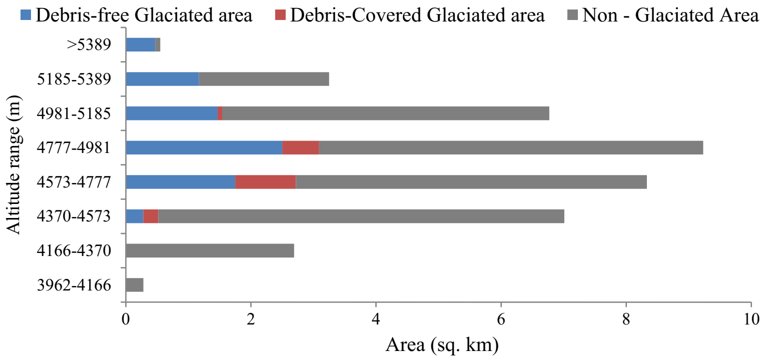

Fig. 2 Hypsometric distribution of land cover for Shaune Garang catchment above discharge gauge (mapped on Landsat 8 image acquired on 20th August, 2014)

4 Estimation of Stream Flow

4.1 Form of Precipitation

It is an important factor affecting surface runoff from both glacierised and non-glacierised area of a catchment. Temperature is the governing factor controlling the form of snow and since the temperature varies with each altitudinal band, the form of precipitation also varies. In the present study, the critical temperature of 2 °C (Singh and Jain 2003; Singh et al. 2008) has been considered in the model to distinguish and estimate the amount of liquid and solid precipitation. It means, if $T_m \geq 2$ °C, the precipitation will be in liquid form contributing directly to the runoff, while if $T_m < 2$ °C, the precipitation will be in solid form and its contribution to stream flow would be delayed.

4.2 Surface Runoff from Glacierised Area

The basic equation (Eq. 2) relating melt with temperature indexed in a unit time can be written as (Hock 2003).

$$M = DDF*T_m \tag{2}$$

Where,

M melt (in mm) for a given time period
DDF degree-day factor (in mm °C^{-1} day^{-1})
T_m mean temperature (in °C)

The discharge contribution from the glacierised area for an altitudinal band can be calculated by using Eq. 3.

$$Q_g = c*[Q_i + Q_s + Q_d + Q_{ri} + Q_{rs} + Q_r] \tag{3}$$

Where,

Q_g is runoff from glacier covered area (m^3 sec^{-1})
c is conversion factor for melt, changing m^3 day^{-1} to m^3 sec^{-1}.

For estimating surface runoff from three different types of surfaces (Q_i, Q_s and Q_d) in a particular altitudinal band can be estimate using Eqs. 4, 5 and 6.

$$Q_i = \frac{[DDF_i * a_i * T_m]}{1000} \tag{4}$$

$$Q_s = \left.\frac{[DDF_s * a_s * T_m}{1000}\right] \tag{5}$$

$$Q_s = \left.\frac{[DDF_d * a_d * T_m}{1000}\right] \tag{6}$$

Where,

Q_i, Q_s and Q_d	are melt contributed by ice, snow and debris surface respectively in m^3 day^{-1}
DDF_i, DDF_s and DDF_d	are degree-day factor calculated for ice, snow and debris-covered surface respectively in mm °C^{-1} day^{-1}
a_i, a_s and a_d	are area covered by ice, snow and debris for the altitudinal band (m^2)
T_m	is temperature specific for altitudinal band calculated using lapse rate (°C).

Apart from melt caused by temperature, another contributor to surface runoff of a glacierised area, is melt by heat transfer from rain to snow and ice surfaces. Rainfall on snow and ice surface during ablation season is very common in Himalaya and contributes significantly to the total runoff. In the present study, this has been calculated using Eqs. 7 and 8 (Singh 2001).

$$Q_{ri} = c * \frac{Q_p}{[\rho * h_f * B]} * a_i \tag{7}$$

$$Q_{rs} = c * \frac{Q_p}{[\rho * h_f * B]} * a_s \tag{8}$$

Where,

Q_{rs} is melt contributed by rainfall on snow surface (m^3 sec^{-1})
Q_{ri} is melt contributed by rainfall on ice surface (m^3 sec^{-1})
c is conversion factor for melt, changing m^3 day^{-1} to m^3 sec^{-1}
ρ is density of water (1000 kg m^{-3})
h_f is Latent heat of fusion of water (335 kJ kg^{-1})
B is Thermal quality of surface (for snow, $B = 0.95$–0.97 and for ice, $B = 1$)

Q_p is energy supplied to the surface by rain (kJ m^{-2} day^{-1}) which has been calculated using Eq. 9

$$Q_p = \frac{\left[\rho * C_p * P_r (T_r - T_s)\right]}{1000} \tag{9}$$

Where,

C_p is specific heat of water (4.2 kJ m^{-2} °C^{-1})
P_r is amount of rain (mm)
T_r is temperature of rain (°C) for which mean air temperature has been taken in present study
T_s is temperature of snow/ice surface which has been considered to be 0 °C in present study
Q_r is runoff contributed by liquid precipitation (m^3) which can be calculated using Eq. 10.

$$Q_r = \left[\frac{P_r * a_f}{1000}\right] \tag{10}$$

Where,

Q_r is runoff contributed by rainfall in glacier covered area (m^3 sec^{-1})
P_r is total rainfall (mm)
a_f is total glacier covered area in the elevation band (m^2)
c is conversion factor for runoff, changing m^3 day^{-1} to m^3 sec^{-1}.

The total runoff from glacierised area of the catchment was estimated by adding Q_g from all the elevation zones.

4.3 Estimation of Runoff from Glacier Free Area

There are three sources of runoff from glacier free area which are considered in the present study. The first source is melt contribution from seasonal snow cover (Q_s') in glacier free area which is calculated by the Eq. 5 used for estimation of discharge from snow covered area on glacier (Q_s). The second source is melt caused by liquid precipitation on snow covered area (Q_{rs}') in the non-glacierised part of the catchment, which is calculated by the Eq. 8 used for calculation of Q_{rs}. Third is rainfall Q_r', which is calculated for a given elevation zone by following the Eq. 10 used for calculation of Q_r.

The total runoff contributing from the non-glacierised area (Q_f) (m^3 sec^{-1}) in the basin can be calculated by using Eq. 11.

$$Q_f = Q_r^{'} + Q_{rs}^{'} + Q_s^{'} \tag{11}$$

4.4 Estimation of Total Stream Flow from the Catchment

Apart from the surface runoff, groundwater also contributes to the discharge at the outlet of the catchment. This is also known as base flow, and needs long term continuous discharge measurement in the catchment for its computation (Subramanya 1994). Due to unavailability of continuous long term daily discharge measurement in the catchment, the average flow measured during 12th to 15th February, 2015 has been considered as the base flow (Q_b=0.27 m^3 sec^{-1}) in present study. Therefore, total discharge in the basin Q (m^3 sec^{-1}) can be calculated by using Eq. 12.

$$Q = Q_g + Q_f + Q_b \tag{12}$$

The loss caused by evaporation and sublimation, and the delay caused by infiltration of melt water and rainfall is not considered here due to insufficient data, which is one of the limitations of the study.

4.5 Estimation of Mass Balance

The Eq. 13 is used to estimate the mass balance of the glacierised part in the catchment in a hydrological year (October-September of following year).

$$MB = A_c - A_b \tag{13}$$

Where,

MB is specific Mass balance (m we)
A_c is total solid precipitation on the glacierised part of the catchment (m)
A_b is summation of total melt from glaciered covered part of the catchment (m) calculated using Eq. 14

$$A_b = \sum \frac{Q_i}{a_i} + \sum \frac{Q_s}{a_s} + \sum \frac{Q_d}{a_d} + \sum \frac{Q_{rs}}{a_s} + \sum \frac{Q_{ri}}{a_i} \tag{14}$$

$\sum \frac{Q_i}{a_i}$ Sum of ice melt from each elevation band in a hydrological year (m)
$\sum \frac{Q_s}{a_s}$ Sum of snow melt of glacier-covered area from each elevation band in a hydrological year (m)
$\sum \frac{Q_d}{a_d}$ Sum of ice melt of debris-covered glacierised area from each elevation band in a hydrological year (m)
$\sum \frac{Q_{rs}}{a_s}$ Sum of snow melt caused by rain on snow covered part of glacier from each elevation band in a hydrological year (m)
$\sum \frac{Q_{ri}}{a_i}$ Sum of ice melt caused by rain on ice from each elevation band in a hydrological year (m)

5 Results and Discussion

The study successfully simulated the runoff for the catchment. In addition, we were able to simulate the mass balance for the glacierised part of the catchment during the years of available precipitation observations. The results of this study are discussed in the sections below.

5.1 Degree-Day Factor (DDF)

The stake measurements were taken on the glacier during ablation season of 2014. Bamboo stakes were installed on the snow surface (during early ablation season), ice surface and debris-covered ice surface using Heucke steam-driven ice drill (Heucke 1999). A large part of the glacier is covered by debris during most of the ablation season, with thickness ranging from thin dirt to big boulders of up to few meters. Therefore, stakes were installed on the ice surface with varying debris-cover at different elevations (Table 2). The stakes were monitored daily from 2nd June 2014 to 25th September, 2014 with few data gaps. As suggested by Hock (2003), the relation of air temperature extrapolated using temperature gradient for particular altitudinal band and ablation was used for calculating the DDF. The mean of the ablation observed was used for calculating DDF for debris-covered ice, debris-free ice and snow-covered area. Since heterogeneity in estimation of DDF for debris-covered part of the glacier was high, the model incorporates different DDF calculated for different altitudinal bands. The DDF for debris-covered part of the glacier has been observed to be increasing with altitude, caused by decrease in debris thickness. Since, the debris thickness was observed to be similar within an altitudinal band, for each altitudinal zone, a single representative DDF value was calculated. The DDF calculated for different surfaces, details of data used for the calculation of DDF with number of stake position observed, and resulting data points have been summarized in Table 2.

5.2 Validation of the Model

The model used in the study for computation of stream flow in Shaune Garang catchment was validated against the daily observed discharge from 11 July 2014 to 27 September 2014 with few data gaps (Fig. 3a and b). In general, the simulated and observed discharge hydrograph matches well with coefficient of determination (R^2) of 0.90. The root mean square error (RMSE) in estimated average discharge of 7.70 is 1.05 $m^3\ sec^{-1}$for the entire validation period, as compared to the mean observed discharge of 8.15 $m^3\ sec^{-1}$. During validation of the model, we observed overestimation in the simulated stream-flow on days of high precipitation. On the remaining days of the validation period, the model was found to give a continuous underestimation of the discharge. The storage capacity of the basin and the contribution in discharge

Table 2 Details of in-situ observed data used for calculation of DDF and the estimated values used in the model

Surface type	Density kg m^{-3}	Number of stake positions monitored	Elevation range (m)	Number of data points	DDF mm °C^{-1} day^{-1}
Snow	550	1	4812	6	5.1 ± 0.3
Ice	890	3	4370–5185	91	8.1 ± 0.2
Debris covered	890	1	4981–5185	24	9.3 ± 0.3
Debris covered	890	1	4777–4981	24	5.2 ± 0.25
Debris covered	890	2	4573–4777	57	3.8 ± 0.8
Debris covered	890	2	4370–4573	42	2.6 ± 0.4

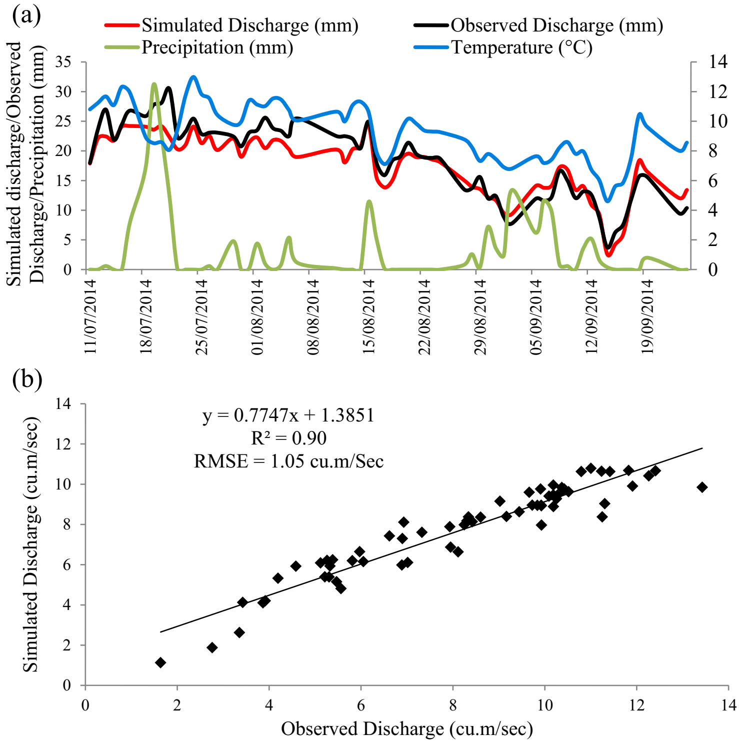

Fig. 3 Comparison of (**a**) Observed discharge and simulated discharge with mean daily temperature and daily total precipitation and (**b**) Observed Discharge and Simulated Discharge in the basin for the validation period

through groundwater flow can be considered as one of the probable reasons for the underestimation by the model.

5.3 Estimation of Long Term Monthly Discharge

The discharge of the catchment for 24 years (1985–2008) was reconstructed using the model. The temporally varying input parameters for monthly discharge estimation were monthly mean temperature, monthly total precipitation and area covered by different surface features.

Figure 4a and b shows the simulated monthly discharge from 1985 to 2007 for Shaune Garang catchment in comparison to mean monthly temperature and precipitation. The figure shows strong exponential relation of simulated discharge with temperature while relationship with total monthly precipitation is not significant. It establishes the fact that the simulated discharge primarily depends on the temperature change.

Shaune Garang glacier is one of the best monitored glaciers in the Indian Himalayan Region in terms of glaciological mass balance and melt season discharge. The average of melt season (May-September) of simulated discharge data from 1985 to 2007 is compared with average melt season discharge measured (Raina et al. 2008) from 1983 to 1989 (Fig. 5).

The simulated discharge is significantly high as compared to the observed discharge during early years of simulation period. As already mentioned, the model works satisfactorily during

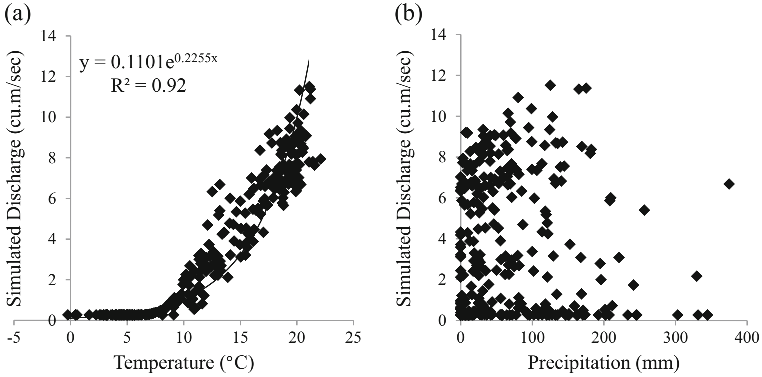

Fig. 4 Comparison of long term monthly simulated discharge with (**a**) mean monthly temperature and (**b**) monthly sum of precipitation

the validation period as we are using station observed precipitation inputs for that period. But during the simulation period 1985–2000, overestimation is caused primarily due to use of APHRODITE data. The linear trend line in Fig. 5 shows decreasing simulated melt season discharge. There might be two probable reasons for decreasing trend of discharge in the basin. The first is high precipitation estimates of APHRODITE data used during first 16 years of simulation (1985–2000) and the second is temporally decreasing glacierised area in the catchment.

The proportion of contribution from different components to total discharge of Shaune Garang catchment is analysed from the simulation output. The analysis shows that seasonal snow melt from glacierised and glacier free part of the catchment is the highest contributor to the total discharge with maximum contribution during June. The average contribution of snow melt to the total discharge was estimated to be more than 30 % during the entire simulation period. The ice melt also shows very significant contribution (29 %) with maximum contribution during July.

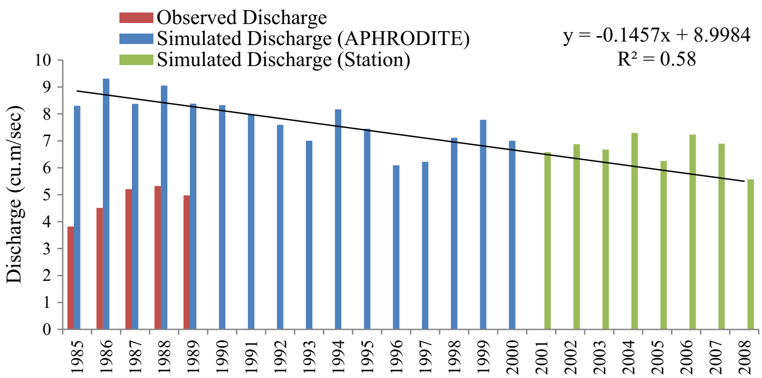

Fig. 5 Comparison of observed melt season discharge (*red bar*) with simulated mean melt season discharge using bias-corrected APHRODITE precipitation data (*blue bar*) and Chhitkul station precipitation data (*green bar*)

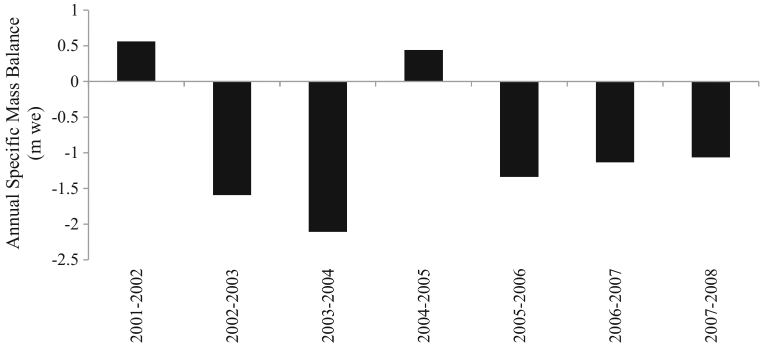

Fig. 6 Mass balance simulated for glaciated region in the Shaune Garang catchment from 2000–01 to 2007–08

5.4 Estimation of Annual Specific Mass Balance

Due to significantly high estimates of total monthly precipitation during winter in the bias-corrected APHRODITE data used during the simulation period 1985–2000, the reconstructed mass balance shows continuous mass gain by the glacierised region in the catchment. Therefore, the mass balance estimated for simulation period 2001–2008 is a true representative of the model outcomes as the temperature and precipitation input data used for this period was collected near the catchment and model shows good performance with in situ observed input parameters (Fig. 3a and b). The mass balance simulation shows average mass loss of 0.89 m we per year during the 7 years of simulation with slight mass gain during hydrological year 2000–01 and 2004–05 (Fig. 6). The result is in accordance with other studies of mass balance measurements using different methods in western Himalayan region. The specific glacier wide mass balance of Chhota Shigri glacier in the Himachal Himalaya, monitored using glaciological method, shows average mass loss of 0.67 m we per year with slight mass gain during hydrological year 2004–05, 2008–09 and 2009–10 (Azam et al. 2012). The geodetic mass balance of nearby Lahaul and Spiti region shows mass loss at the rate of 0.44 ± 0.09 m we per year for the period 1999–2011 (Vincent et al. 2013).

5.5 Comparison of Simulated Discharge and Simulated Mass Balance

Analysis of annual net mass balance and average melt season discharge in the Indian Himalayan Region for four well-studied glaciers, including Shaune Garang, for around 23 years show high discharge during more positive mass balance years (Thayyen and Gergan 2010; Singh et al. 2016). Our study supports this conclusion by comparing the simulated mass balance and average melt season discharge for respective hydrological years (Fig. 7). It is obvious that during the years of positive mass balance, the amount of solid precipitation is higher in the basin. As per our understanding, the reason of higher discharge during years of more positive mass balance can be attributed to the contribution of seasonal snow melt from glacier free area of the catchment.

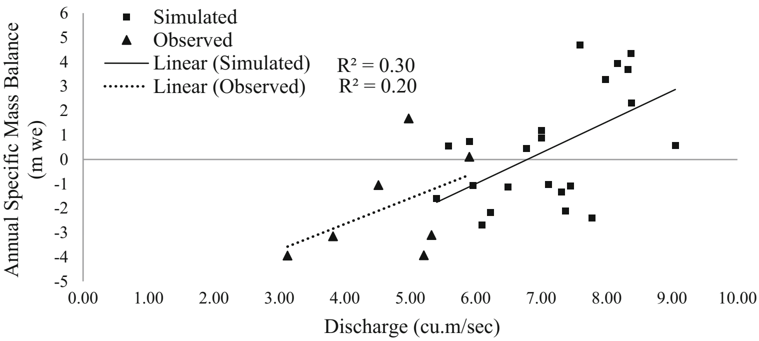

Fig. 7 Comparison of mass balance and discharge for observation (1982–83 to 1988–89) (Raina et al. 2008) and simulation (1985–86 to 2007–08)

6 Conclusions

The estimation of discharge contributed by a glacierised basin is complicated due to change in storage and drainage properties of the basin during ablation season. In addition, liquid precipitation on glaciers (in present case, up to altitudinal band 5135–5389 m asl during maximum temperature months as per the model results) is a common situation in the Himalaya that further exaggerates the problem of modelling the stream-flow. We have used degree-day approach to model stream-flow and its different components. The degree-day factors for different land covers were found to be between 2.6 ± 0.4 and 9.3 ± 0.3 mm°C^{-1}day^{-1}, with decrease in degree-day factor for debris-covered part of glacier with altitude. The model was established and validated using in situ measurements carried out in the field. After validation, the model was used to simulate long term mean monthly stream-flow (1985–2008) and mass balance (2001–2008). The temporal land cover mapping of the catchment suggested a decrease in the glacierised area and an increase in the debris-cover proportion during the simulation period. The simulation results show an overall decreasing trend during the period of simulation. The reconstructed mass balance is in accordance with the past studies in the region and shows a continuous loss of mass with slight mass gain during 2001–02 and 2004–05. The simulated discharge shows insignificant positive correlation with net annual mass balance and is in agreement with the past observations for several other glaciers in the Indian Himalayan region.

We, for the first time, report degree-day factors (separately for snow, ice and supraglacial debris) for Shaune Garang glacier, and for different altitudinal zones of any Himalayan glacier, estimated using daily stake measurements. Also, our study presents the first-hand account of reconstruction of mass balance and discharge of a Himalayan glacier using a glacio-hydrological model. In addition, we are improving the model robustness and performance by including temporally varying snow-cover, glacier area and debris cover observations, derived from remotely sensed data. The overall analysis shows the applicability of temperature index-based glacio-hydrological model for estimation of stream-flow and mass balance in a Himalayan catchment with debris-covered glaciers. The premise of this study is not based on the utilization of reanalysis data, but it is based on the incorporation of in situ observations and remote sensing inputs in the model. When we are using in situ data, the acceptable performance of the model is an indicative of the fact that it is working satisfactorily for debris-covered glaciers. The incorporation of reanalysis data is just an add-on to highlight the problems in case of future use of such data for running our model in data-deficient Himalayan region.

Acknowledgments The study is a part of internationally coordinated project entitled "Contribution to High Asia Runoff from Ice and Snow (CHARIS) https://nsidc.org/charis/" funded by United States Agency for International Development (USAID). The authors are grateful to Bhakhra Beas Management Board (BBMB) and Dr. Hendrik Wulf, University of Zurich, Switzerland for providing meteorological data of Rakchham and Chhitkul. The support provided by Mr. Vinod Negi, Rakchham, H.P. in carrying out field work is deeply acknowledged. We would also like to thank Dr. George P. Tsakiris, Chief Editor, Water Resources Management and two anonymous reviewers for the comments which significantly improved the quality of the manuscript.

References

Andermann C, Stephane B, Richard G (2011) Evaluation of precipitation data sets along the Himalayan front. Geochem Geophys Geosyst 12(7):Q07023. doi:10.1029/2011GC003513

Archer DR, Fowler HJ (2004) Spatial and temporal variations in precipitation in the upper Indus basin, global teleconnections and hydrological implications. Hydrol Earth Syst Sci 8:47–61. doi:10.5194/hess-8-47-2004

Arora M, Singh P, Goel NK, Singh RD (2006) Spatial distribution and seasonal variability of rainfall in a mountainous basin in the Himalayan region. Water Resour Manag 20(4):489–508. doi:10.1007/s11269-006-8773-4

Arora M, Singh P, Goel NK, Singh RD (2008) Climate variability influences on hydrological responses of a large Himalayan basin. Water Resour Manag 22(10):1461–1475. doi:10.1007/s11269-007-9237-1

Azam MF, Wagnon P, Ramanathan AL, Vincent C, Sharma P, Arnaud Y, Linda A, Pottakkal JG, Chevallier P, Singh VB, Berthier E (2012) From balance to imbalance: a shift in the dynamic behaviour of Chhota Shigri glacier, western Himalaya, India. J Glaciol 58(208):315–324. doi:10.3189/2012JoG11J123

Azam MF, Wagnon P, Vincent C, Ramanathan AL, Favier V, Mandal A, Pottakkal JG (2014a) Processes governing the mass balance of Chhota Shigri Glacier (western Himalaya, India) assessed by point-scale surface energy balance measurements. Cryosphere 8:2195–2217. doi:10.5194/tc-8-2195-2014

Azam MF, Wagnon P, Vincent C, Ramanathan AL, Linda A, Singh VB (2014b) Reconstruction of the annual mass balance of Chhota Shigri glacier, Western Himalaya, India, since 1969. Ann Glaciol 55(66):69–80. doi:10.3189/2014AoG66A104

Bajracharya SR, Shrestha B (eds) (2011) The status of glaciers in the Hindu Kush-Himalayan region. International Centre for Integrated Mountain Development (ICIMOD), Kathmandu

Basistha A, Arya DS, Goel NK (2008) Spatial distribution of rainfall in Indian Himalayas—a case study of Uttarakhand region. Water Resour Manag 22(10):1325–1346. doi:10.1007/s11269-007-9228-2

Bhutiyani MR, Kale VS, Pawar NJ (2007) Long-term trends in maximum, minimum and mean annual air temperatures across the Northwestern Himalaya during the twentieth century. Clim Change 85(1):159–177. doi:10.1007/s10584-006-9196-1

Bhutiyani MR, Kale VS, Pawar NJ (2010) Climate change and the precipitation variations in the Northwestern Himalaya: 1866–2006. Int J Climatol 30(4):535–548. doi:10.1002/joc.1920

Bøggild CE, Reeh N, Oerter H (1994) Modelling ablation and mass-balance sensitivity to climate change of Storstrømmen, northeast Greenland. Global Planet Change 9(1–2):79–90. doi:10.1016/0921-8181(94)90009-4

Bolch T, Kulkarni AV, Kääb A, Huggel C, Paul F, Cogley JG, Frey H, Kargel JS, Fujita K, Scheel M, Bajracharya S, Stoffel M (2012) The state and fate of Himalayan glaciers. Science 336(6079):310–314. doi:10.1126/science.1215828

Bookhagen B, Burbank DW (2010) Toward a complete Himalayan hydrological budget: spatiotemporal distribution of snowmelt and rainfall and their impact on river discharge. J Geophys Res 115:F03019. doi:10.1029/2009jf001426

Braithwaite RJ, Zhang Y (1999) Modelling changes in glacier mass balance that may occur as a result of climate changes. Geogr Ann Ser A Phys Geogr 81(4):489–496. doi:10.1111/1468-0459.00078

Cea C, Cristóbal J, Pons X (2007) An improved methodology to map snow cover by means of Landsat and MODIS imagery. IEEE Int Geosci Remote Sens Symp (IGRASS) pp 4217–4220

Dimri AP, Dash SK (2012) Wintertime climatic trends in the Western Himalaya. Clim Change 111(3–4):775–800. doi:10.1007/s10584-011-0201-y

Fujita K, Ageta Y (2000) Effect of summer accumulation on glacier mass balance on the Tibetan Plateau revealed by mass balance model. J Glaciol 46(153):244–252. doi:10.3189/172756500781832945

Gardelle J, Berthier E, Arnaud Y, Kääb A (2013) Region-wide glacier mass balances over the Pamir–Karakoram–Himalaya during 1999–2011. Cryosphere 7(4):1263–1286. doi:10.5194/tc-7-1263-2013

Garg V, Jothiprakash V (2012) Sediment Yield Assessment of a Large Basin using PSIAC Approach in GIS Environment. Water Resour Manag 26(3):799–840. doi:10.1007/s11269-011-9945-4

Gudmundsson L, Bremnes JB, Haugen JE, Engen-Skaugen T (2012) Technical note: downscaling RCM precipitation to the station scale using statistical transformations—a comparison of methods. Hydrol Earth Syst Sci 16:3383–3390. doi:10.5194/hess-16-3383-2012

Hall DK, Riggs GA (2007) Accuracy assessment of the MODIS snow products. Hydrol Process 21(12):1534–1547. doi:10.1002/hyp.6715

Herschy R (1993) The velocity-area method. Flow Meas Instrum 4(1):7–10. doi:10.1016/0955-5986(93)90004-3

Heucke E (1999) A light portable steam-driven ice drill suitable for drilling holes in ice and firn. Geogr Ann Ser A Phys Geogr 81(4):603–609. doi:10.1111/1468-0459.00088

Hock R (2003) Temperature index melt modelling in mountain areas. J Hydrol 282(1–4):104–115. doi:10.1016/S0022-1694(03)00257-9

Immerzeel WW, Van Beek LPH, Bierkens MFP (2010) Climate change will affect the Asian water towers. Science 328:1382–1385. doi:10.1126/science.1183188

Jain SK, Singh P, Saraf AK, Seth SM (2003) Estimation of sediment yield for a rain, snow and glacier fed river in the Western Himalayan region. Water Resour Manag 17(5):377–393. doi:10.1023/A:1025804419958

Jain SK, Goswami A, Saraf AK (2009) Role of elevation and aspect in snow distribution in Western Himalaya. Water Resour Manag 23(1):71–83. doi:10.1007/s11269-008-9265-5

Jain SK, Goswami A, Saraf AK (2010) Assessment of snowmelt runoff using remote sensing and effect of climate change on runoff. Water Resour Manag 24(9):1763–1777. doi:10.1007/s11269-009-9523-1

Juen M, Mayer C, Lambrecht A, Han H, Liu S (2014) Impact of varying debris cover thickness on ablation: a case study for Koxkar Glacier in the Tien Shan. Cryosphere 8(2):377–386. doi:10.5194/tc-8-377-2014

Kääb A, Berthier E, Nuth C, Gardelle J, Arnaud Y (2012) Contrasting patterns of early twenty-first-century glacier mass change in the Himalayas. Nature 488(7412):495–498. doi:10.1038/nature11324

Kayastha RB, Ohata T, Ageta Y (1999) Application of mass balance model to a Himalayan glacier. J Glaciol 45:559–567

Krakauer NY, Pradhanang SM, Lakhankar T, Jha AK (2013) Evaluating satellite products for precipitation estimation in mountain regions: a case study for Nepal. Remote Sens 5:4107–4123. doi:10.3390/rs5084107

Lejeune Y, Bertrand JM, Wagnon P and Samuel M (2013) A physically based model of the year-round surface energy and mass balance of debris-covered glaciers. J Glaciol 59(214):327–344. doi:10.3189/2013JoG12J149

Li H, Xu C-Y, Beldring S, Tallaksen LM, Jain SK (2015) Water resources under climate change in Himalayan basins. Water Resour Manag. doi:10.1007/s11269-015-1194-5

Liu X, Chen B (2000) Climatic warming in the Tibetan plateau during recent decades. Int J Climatol 20(14):1729–1742. doi:10.1002/1097-0088(20001130)20:14<1729::AID-JOC556>3.0.CO;2-Y

Lutz AF, Immerzeel WW, Shrestha AB, Bierkens MFP (2014) Consistent increase in High Asia's runoff due to increasing glacier melt and precipitation. Nat Clim Chang 4:587–592. doi:10.1038/nclimate2237

Mayewski PA, Jeschke PA (1979) Himalayan and Trans-Himalayan glacier fluctuations since Ad 1812. Arct Alp Res 11(3):267–287

Mölg T, Maussion F, Yang W, Scherer D (2012) The footprint of Asian monsoon dynamics in the mass and energy balance of a Tibetan glacier. Cryosphere 6:1445–1461. doi:10.5194/tc-6-1445-2012

Nicholson L, Benn DI (2006) Calculating ice melt beneath a debris layer using meteorological data. J Glaciol 52(178):463–470. doi:10.3189/172756506781828584

Ohmura A (2001) Physical basis for the temperature-based melt index method. J Appl Meteorol 40(4):753–761. doi:10.1175/1520-0450)(2001)040<0753:PBFTTB>2.0.CO;2

Ohmura A, Bauder A, Müller H, Kappenberger G (2007) Long term change of mass balance and the role of radiation. Ann Glaciol 46:367–374. doi:10.3189/172756407782871297

Panday PK, Christopher AW, Frey KE, Brown ME (2014) Application and evaluation of a snowmelt runoff model in the Tamor River basin, Eastern Himalaya using a Markov Chain Monte Carlo (MCMC) data assimilation approach. Hydrol Process 28(21):5337–5353. doi:10.1002/hyp.10005

Pandey P, Venkataraman G (2013) Changes in the glaciers of Chandra-Bhaga basin, Himachal Himalaya, India, between 1980 and 2010 measured using remote sensing. Int J Remote Sens 34(15):5584–5597. doi:10.1080/01431161.2013.793464

Pradhananga NS, Kayastha RB, Bhattarai BC, Adhikari TR, Pradhan SC, Devkota LP, Shrestha AB, Mool PK (2014) Estimation of discharge from Langtang River basin, Rasuwa, Nepal, using a glacio-hydrological model. Ann Glaciol 55(66):223–230. doi:10.3189/2014AoG66A123223

Pratap B, Dobhal DP, Mehta M, Bhambri R (2015) Influence of debris cover and altitude on glacier surface melting: a case study on Dokriani Glacier, Central Himalaya, India. Ann Glaciol 56(70):9–16. doi:10.3189/2015AoG70A971

Raina VK, Srivastava D, Singh RK, Sangewar CV (2008) Glacier regimen, fluctuation, hydrometry and mass transfer studies in the Himalayas. In: Raina VK, Srivastava D (eds) Glacier Atlas of India. Geological Society of India, Bangalore, pp 206–216

Schild A (2008) The case of the Hindu Kush–Himalayas: ICIMOD's position on climate change and mountain systems. Mt Res Dev 28(3/4). doi:10.1659/mrd.mp009

Shea JM, Immerzeel WW, Wagnon P, Vincent C, Bajracharya S (2015) Modelling glacier change in the Everest region, Nepal Himalaya. Cryosphere 9(3–3):1105–1128. doi:10.5194/tc-9-1105-2015

Shrestha AB, Wake CP, Mayewski PA, Dibb JE (1999) Maximum temperature trends in the Himalaya and its vicinity: an analysis based on temperature records from Nepal for the period 1971–94. J Climate 12:2775–2767. doi:10.1175/1520-0442(1999)012%3C2775:MTTITH%3E2.0.CO;2

Shrestha AB, Wake CP, Dibb JE, Mayewski PA (2000) Precipitation fluctuations in the Nepal Himalaya and its vicinity and relationship with some large scale climatological parameters. Int J Climatol 20(3):317–327. doi:10.1002/(SICI)1097-0088(20000315)20:3<317::AID-JOC476>3.0.CO;2-G

Singh P (2001) Hydrological modelling of snow and glacier covered basins. Proc Natl Acad Sci India A 71:195–222

Singh P, Bengtsson L (2003) Effect of warmer climate on the depletion of snow covered area in the Satluj basin in the western Himalayan region. Hydrol Sci J 48(3):413–425. doi:10.1623/hysj.48.3.413.45280

Singh P, Jain SK (2003) Modelling of streamflow and its components for a large Himalayan basin with predominant snowmelt yields. Hydrol Sci J 48(2):257–276. doi:10.1623/hysj.48.2.257.44693

Singh P, Haritashya UK, Kumar N (2008) Modelling and estimation of different components of streamflow for Gangotri Glacier basin, Himalayas. Hydrol Sci J 53(2):309–322. doi:10.1623/hysj.53.2.309

Singh S, Kumar R, Bhardwaj A, Sam L, Shekhar M, Singh A, Kumar R and Gupta A (2016) Changing climate and glacio-hydrology in Indian Himalayan Region: a review. Wiley Interdiscip Rev Clim Change 7(3):393–410. doi:10.1002/wcc.39

Srivastava D, Kumar A, Verma A, Swaroop S (2014) Analysis of climate and melt-runoff in Dunagiri Glacier of Garhwal Himalaya (India). Water Resour Manag 28(10):3035–3055. doi:10.1007/s11269-014-0653-8

Subramanya K (1994) Engineering hydrology, 2nd edn. Tata McGraw-Hill Education, New Delhi

Thayyen RJ, Gergan JT (2010) Role of glaciers in watershed hydrology: a preliminary study of a 'Himalayan catchment'. Cryosphere 4(1):115–128. doi:10.5194/tc-4-115-2010

Tiwari PC, Joshi B (2012) environmental changes and sustainable development of water resources in the Himalayan headwaters of India. Water Resour Manag 26(4):883–907. doi:10.1007/s11269-011-9825-y

Vincent C, Al R, Wagnon P, Dobhal DP, Linda A, Berthier E, Sharma P, Arnaud Y, Azam MF, Jose PG, Gardelle J (2013) Balanced conditions or slight mass gain of glaciers in the Lahaul and Spiti region (northern India, Himalaya) during the nineties preceded recent mass loss. Cryosphere 7(2):569–582. doi:10.5194/tc-7-569-2013

Xu J, Grumbine RE, Shrestha A, Eriksson M, Yang X, Wang Y, Wilkes A (2009) The melting Himalaya: cascading effects of climate change on water, biodiversity, and livelihoods. Conserv Biol 23(3):520–530. doi:10.1111/j.1523-1739.2009.01237.x

Yatagai A, Kamiguchi K, Arakawa O, Hamada A, Yasutom N, Kitoh A (2012) APHRODITE: constructing a long-term daily gridded precipitation dataset for Asia based on a dense network of rain gauges. Bull Am Meteorol Soc 93(9):1401–1415. doi:10.1175/BAMS-D-11-00122.1

Zhang G, Kang S, Fujita K, Huintjes E, Xu J, Yamazaki T, Haginoya S, Wei Y, Scherer D, Schneider C, Yao T (2013) Energy and mass balance of Zhadang glacier surface, central Tibetan Plateau. J Glaciol 59(213):137–148. doi:10.3189/2013JoG12J152